

THE APPLICATION OF LIGHT SCATTERING AND SMALL-ANGLE X-RAY SCATTERING TO INTERACTING BIOLOGICAL SYSTEMS

ABSTRACT

Light scattering and small-angle X-ray scattering are very powerful tools for the study of interactions of biological macromolecules in solution, since both are capable of yielding information on the thermodynamics and the geometry of intramolecular interactions.

A brief review of fluctuation theory as applied to the two techniques is presented. It is shown that in two- and three-component systems identical information on the thermodynamic interactions of the macromolecular solute is obtainable from the two techniques. This is illustrated by examples. Typical patterns of interaction in two-component systems are shown for the cases of an isoionic protein in deionized water, a highly charged protein in deionized water, and a protein undergoing reversible aggregation. The three-component cases illustrated are: interaction of the macromolecule with a small solute molecule, preferential hydration of the macromolecules and formation of specific complexes between two proteins.

Although the geometric information obtainable from the two methods is identical, difference in the degree of resolution makes the two techniques complementary. This is demonstrated by an analysis of the structure of high molecular weight ribonucleic acid by the two scattering techniques, light scattering giving the overall geometry of the molecule, while X-ray scattering yields details of the internal structure; the two sets of data are shown to be mutually consistent. In another example, it is shown how the geometric information obtained by small-angle X-ray scattering on the aggregation of β -lactoglobulin can be used to verify conclusions drawn from a thermodynamic light scattering study.

INTRODUCTION

In the present-day development of molecular biology, interactions between various macromolecules with specific functions are assuming an ever more prominent role. In the mechanisms proposed for protein biosynthesis, various nucleic acid-enzyme-amino acid complexes seem to occupy a key position, enzyme action often involves protein-protein interactions, while the structure of the living cell itself depends very strongly on a complicated network of intermolecular interactions. As a particularly important example, one might cite the case of hemoglobin whose structure, consisting of four molecular

* Eastern Utilization Research and Development Division, Agricultural Research Service, U.S. Department of Agriculture.

units joined together by non-covalent bonds, leads to a system thermodynamically capable of transmitting oxygen absorbed from the atmosphere to various parts of the organism.

The detailed understanding of the functioning of these various systems requires accurate knowledge of thermodynamic and geometric aspects of the interactions involved. This information is often obtained from *in vitro* studies of the isolated systems in a medium resembling their native environment, namely in an aqueous solution which contains a moderate amount of salt ($\Gamma/2 \sim 0.15$).

While a great variety of techniques are available for the study of interactions between biological macromolecules, two methods based upon the scattering of electromagnetic radiation are particularly suited, since they are capable of yielding at once the thermodynamic and the geometric information desired. These are the techniques of light scattering and small-angle X-ray scattering. It is the purpose of this paper to demonstrate by examples how these two techniques can be applied to biological systems in various states of interaction. No attempt will be made at a comprehensive review of the literature on the subject and the examples used will be those with which the author is best acquainted.

The basic theory of scattering has been treated in a number of publications (see, for example, Debye, 1947; Oster, 1948; Tanford, 1961; Kirkwood and Goldberg, 1950; Stockmayer, 1950; Brinkman and Hermans, 1949; Geiduschek and Holtzer, 1958; Timasheff and Kronman, 1958; Timasheff and Coleman, 1960; Guinier and Fournet, 1955; Van de Hulst, 1957; and Flügge, 1957), and will not be presented here in detail.

While the theories of light scattering and small-angle X-ray scattering are essentially identical and the two techniques yield in principle the same information, the two methods are actually complementary. This is due to the difference in the wave lengths of the radiation used (3000–5000 Å in light scattering, 1–5 Å in small-angle X-ray scattering). As a result, light scattering is most useful for the study of the geometry of larger molecules (>1000 Å), while X-ray scattering permits the examination of much smaller molecules (20–1000 Å). For thermodynamic studies, the two methods are interchangeable, with light scattering being preferable in the low concentration range (~ 0.01 –30 g/l), and small-angle X-ray scattering being most useful at high concentrations of the macromolecules (~ 10 –500 g/l).

THERMODYNAMICS OF SCATTERING

When a particle is subjected to an electric field of strength, E , a dipole, p , is induced in it, whose magnitude is given by

where α is the polarizability. The oscillating dipole radiates energy in all directions with an intensity, i_s , which, for the case of n particles, small relative to the wavelength of the radiation, is equal to

$$\frac{i_s}{I_0} = \frac{8\pi^4 n \alpha^2}{\lambda'^2 r^2} (1 + \cos^2 \theta) \quad (2)$$

where I_0 is the intensity of the incident beam, λ' is its wavelength in the medium, r is the distance of the observer from the scattering medium and θ is the angle between the scattered and the incident beams. This is the basic equation of light scattering.

In the case of free electrons, the polarizability can be expressed as

$$\alpha = \frac{-e^2}{4\pi^2 \nu^2 m} \quad (3)$$

where e is the electronic charge, ν is the frequency of the incident radiation and m is the mass of the electron. Properly combining equations (2) and (3), the scattering due to an electron, I_e , is found to be

$$\frac{I_e}{I_0} = \frac{e^4}{2r^2 m^2 c^4} (1 + \cos^2 \theta) \quad (4)$$

where c is the velocity of light. This is the well-known Thomson equation, which forms the basis of small-angle X-ray scattering. The scattering from a particle, which represents the sum of the scattering from its electrons, is given by:

$$i_s = I_e N_e^2 P(\theta) \quad (5)$$

where N_e is the number of electrons in the particle, and $P(\theta)$ is a parameter describing the angular distribution of the scattering; it is a function of the geometry of the particle.

When particles (or molecules) are placed in solution, it can be shown that the excess scattering observed over that of the pure solvent is due to fluctuations in the composition within a volume element δV . The appropriate equations are:

$$\text{Light scattering: } \frac{\Delta i_s}{I_0} = \frac{\pi^2 \delta V}{2(\lambda')^4 r^2} \left(\frac{\partial \epsilon}{\partial C} \right)_{T,p}^2 \overline{\Delta C^2} P(\theta) (1 + \cos^2 \theta) \quad (6a)$$

$$\text{X-ray scattering: } \Delta i_s = I_e \left(\frac{\partial \rho}{\partial C} \right)_{T,p}^2 \delta V \overline{\Delta C^2} P(\theta) \quad (6b)$$

where ϵ is the dielectric constant of the solution, C is the concentration in g/ml, ρ is the density of the solution, expressed in electrons per unit volume.

$\overline{\Delta C^2}$ is the time average of the square of the concentration fluctuations, ΔC^2 , and is related to the chemical potential of the solvent, μ_0 , by

$$\overline{\Delta C^2} = \frac{-kTC\bar{V}_0}{\delta V \left(\frac{\partial \mu_0}{\partial C} \right)_{T,p}} \quad (7)$$

where k is Boltzmann's constant, T is the thermodynamic temperature and \bar{V}_0 is the partial molar volume of the solvent.

Combination of equation (7) with equations (6) leads to the following expression for scattering in a two-component system (solvent: component 0; solute: component 2):

$$K' \left(\frac{\partial n}{\partial C^2} \right)^2 \frac{C_2}{\Delta i(0)} = \frac{1}{M_2} \left[1 + \frac{C_2}{RT} \frac{\partial \mu_2^e}{\partial C_2} \right] = K'' \left(\frac{\partial \rho}{\partial C_2} \right)^2 \frac{C_2}{\Delta i(0)} \quad (8)$$

(light scattering) (X-ray scattering)

$$\mu_2 = RT \log C_2 + \mu_2^e + \mu_2^0(T, p)$$

where K , and K'' are constants, R is the gas constant, M_2 is the molecular weight of the solute, n is the refractive index of the solution, $\Delta i(0)$ is the excess scattering intensity over that of pure solvent, extrapolated to zero angle*, and μ_2^e is the excess chemical potential of the solute, equal to $RT \log \gamma_2$, where γ_2 is the activity coefficient of component 2.

The fluctuation theory can be extended also to systems of several components. For a three-component system (solvent: component 0, macromolecule: component 2, third component, such as supporting electrolyte: component 1), the scattering is described (using the notation of Kirkwood and Goldberg (1950)) by:

$$K' \left(\frac{\partial n}{\partial C_2} \right)^2 \frac{C_2}{\Delta i(0)} \text{ (light scattering)} = K'' \left(\frac{\partial \rho}{\partial C_2} \right)^2 \frac{C_2}{\Delta i(0)} \text{ (X-ray scattering)}$$

$$= \frac{1}{(1+D)} \left\{ \frac{1}{M_2} + \left[\frac{A_{22}}{M_2} - \frac{A_{12}}{M_1} \left(\frac{A_{12}}{\Sigma v_1 + A_{11}} \right) \right] C_2 \right\}$$

$$D = \frac{-2\alpha A_{12}}{\Sigma v_1 + A_{11}} + \left(\frac{\alpha A_{12}}{\Sigma v_1 + A_{11}} \right)^2 ; \quad A_{ij} = \frac{1}{RT} \frac{\partial \mu_i^{(e)}}{\partial C_j} \quad (9)$$

$$\alpha = (\partial n / \partial C_1)_{C_2} / (\partial n / \partial C_2)_{C_1} \text{ (light scattering)}$$

$$\alpha = (\partial \rho / \partial C_1)_{C_2} / (\partial \rho / \partial C_2)_{C_1} = \frac{Q_1 (1 - \rho_0 \bar{V}_1 / Q_1)}{Q_2 (1 - \rho_0 \bar{V}_2 / Q_2)} \text{ (X-ray scattering)}$$

* The excess scattering of light is often expressed as the Rayleigh ratio, $R_\theta = i(\theta)r^2 / I_0(1 + \cos^2 \theta)$, or the turbidity, $\tau = (16\pi/3)/R_\theta$. $i(\theta)$ is the scattering increment at angle θ .

When Σv_1 is the number of particles into which component 1 dissociates, Q_i is the number of electrons in a molecule of component i divided by its mass in grams, ρ_i is the density in electrons per cm^3 and \bar{V}_i is the partial specific volume of unhydrated component i , in cm^3 per electron.

This brief outline of the fluctuation theory makes it evident that the equations of light scattering and small-angle X-ray scattering are essentially identical, the refractive increment in light scattering being replaced by the density increment in X-ray scattering. Thus, the two methods are capable of yielding identical thermodynamic information. Closer examination of equations (8) and (9) shows that, while in a two-component system the molecular weight of the solute is obtained directly by extrapolation to zero concentration and all interactions are expressed by the concentration dependent term, in a three-component system, extrapolation yields the product of the molecular weight with a compositional parameter α and a parameter describing thermodynamic interactions between components 2 and 1. This fact may be used to advantage in investigating the interactions of two solutes. We will show now by a few examples how equations 8 and 9 can be used to characterize various types of interactions.

Two-Component Systems

First we shall summarize briefly the effect of various interactions of component 2 with itself on the shape of the scattering curve. While equation (8) describes exactly the scattering in a two-component system, for a polyelectrolyte, such as a protein, the coefficient of the concentration dependent term may itself have a complicated concentration dependence and result in various complex shapes of the curve. Three distinct cases may be described:

1. *Isoionic protein in ion-free water.* The principal interactions are those due to proton fluctuations and to progressive ionization of the protein (Kirkwood and Timasheff, 1956). The concentration dependent term of equation (8) assumes the form:

$$\frac{C_2}{RT} \frac{\partial \mu_2^e}{\partial C_2} = \frac{C_2}{M_2} \left(-\frac{\pi N e^4 \langle Z_2^2 \rangle_{Av}^2}{(\epsilon k T)^2 \kappa (1 + \kappa a)^2} + \frac{7}{6} \pi N a^3 + \frac{\bar{Z}_2^2}{[\text{H}^+]} \frac{1}{[\text{H}^+] + K_w/[\text{H}^+]^2 - \frac{m_2}{2.303[\text{H}^+]} \frac{d\bar{Z}_2}{d\text{pH}} + 2B'} \right) \quad (10)$$

$$\kappa^2 = \frac{4\pi N e^2}{\epsilon k T} \left(\frac{\langle Z_2^2 \rangle_{Av} C_2}{M_2} \right)$$

where $\langle Z_2^2 \rangle_{Av}$ is the mean square charge of the protein in protonic units, e , ϵ is the dielectric constant of the medium, k is Boltzmann's constant, κ and

a are the Debye-Hückel parameters, N is Avogadro's number, \bar{Z}_2 is the average charge of the protein, $[H^+]$ is the hydrogen ion concentration, K_w is the water dissociation constant, and m_2 is the molar concentration of component 2. The first term in concentration which represents the contribution of charge fluctuations on the protein molecule, in the limit, is linear in the square root of protein concentration; the second term is the excluded volume and is linear in the first power of protein concentration; the third term, which reflects the ionization of protein with dilution, is a function which passes through a maximum at very low values of protein concentration; $2B'$ reflects the combined effect of all other types of intermolecular force. The typical concentration dependence curve is shown as curve 1 of Fig. 1.

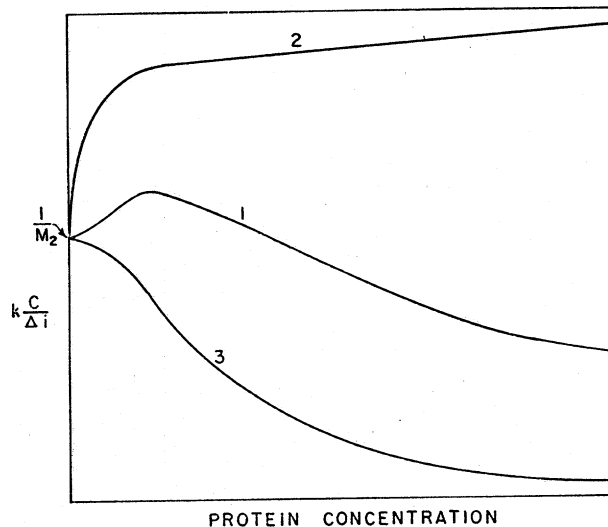


FIG. 1. Two component scattering curves. 1. Isoionic protein in ion-free water; 2. Highly charged protein in ion-free water; 3. Associating protein. (Both coordinates are in arbitrary units.)

The net result of these interactions is an attraction between solute molecules; its magnitude may be determined by scattering measurements, using equation (10) (Timasheff, Dintzis, Kirkwood and Coleman, 1957).

2. *Protein systems with high charge in ion-free water.* In this case, strong electrostatic forces result in ordering of solute molecules in the solution. This leads to intermolecular interference of the scattering, and can be treated as an interference phenomenon (Fournet, 1951; Doty and Steiner, 1952). A typical curve obtained is drawn in Fig. 1 (curve 2). This particular case will not be described in detail here and the reader is referred to the cited literature.

3. *Macromolecule undergoing a reversible aggregation ($nP \rightleftharpoons P_n$).* While such systems are normally examined in the presence of supporting electrolyte,

in most cases they can be treated as pseudo two-component systems. Here, the coefficient of the concentration dependent term may be decomposed into the product of two contributing effects, one representing the association, the other accounting for other thermodynamic interactions:

$$\frac{1}{RT} \frac{\partial \mu_2^{(e)}}{\partial C_2} = \frac{\partial \log \gamma'_2}{\partial C_2} + \frac{\partial \log f_2}{\partial C_2}$$

$$\frac{\partial \log f_2}{\partial C_2} = - \frac{Kn(n-1)f_2^n C_2^{n-2}}{M_2^{n-1}f_2 + Kn^2 f_2^n C_2^{n-1}} = \frac{1}{C_2} \left(\frac{M_2 - \bar{M}_w}{\bar{M}_w} \right) \quad (11)$$

$$K = \frac{(1-f_2)M_2^{n-1}}{nf_2^n C_2^{n-1}}$$

where M_2 is the monomer molecular weight, \bar{M}_w is the weight average molecular weight at concentration C_2 , f_2 is the fraction of component 2 not aggregated and γ'_2 is its activity coefficient. Curve 3 of Fig. 1 represents typical experimental results obtained in this case. This particular curve was taken from a study of the tetramerization of β -lactoglobulin A, in which both scattering techniques were used giving essentially overlapping results (Townend and Timasheff, 1960; Timasheff, Witz and Luzzati, in preparation).

Three-component Systems

In a three-component system, the situation becomes somewhat more complicated, since both the concentration dependent term and the extrapolated term are now functions of interactions between components 1 and 2. This makes it possible, however, to measure the degree of interaction between these two components. Three examples will be treated: (1) Interaction between a macromolecular component 2 and small component 1, i.e. binding of 1 to 2; (2) Preferential binding of component 0 to component 2, i.e., the degree of hydration; (3) Complex formation between two proteins, P and S , according to the reaction $P + nS \xrightleftharpoons{K} PS_n$, where P is component 2 and S component 1.

Case 1: Binding of small molecules. The factor D of equation (9) can be expressed as:

$$D = 2\alpha \frac{M_1}{M_2} \frac{\bar{v}}{\Sigma v_1} + \left(\alpha \frac{M_1}{M_2} \frac{\bar{v}}{\Sigma v_1} \right)^2 \quad (12)$$

where \bar{v} is the average number of particles of component 1 bound to a molecule of component 2.

Using binding data from the literature (Scatchard, Coleman and Shen, 1957; Kay and Edsall, 1956; Katz, 1952), values of D have been calculated for serum albumin (BSA) in the presence of NaCl, NaSCN and urea, and of sodium DNA'ate in the presence of $HgCl_2$. Results of the calculations for light scattering and small-angle X-ray scattering are summarized in Table 1.

TABLE 1. EFFECT OF BINDING OF SMALL MOLECULES ON EXTRAPOLATION IN LIGHT SCATTERING AND SMALL-ANGLE X-RAY SCATTERING

(1) Macromolecule	(2) Component 1	(3) $C_1, \text{g/ml} \times 10^3$	(4) $A_{12}^{(a)}$ ml/g	(5)		(6)		(7)		(8)		(9)		(10)	
				α	$D \times 10^3$	Light scattering ^(b) $M_2, \text{app}/M_2, \text{real}$	$M_2, \text{app}/M_2, \text{real}$	z	$D \times 10^3$	X-ray scattering ^(b) $M_2, \text{app}/M_2, \text{real}$	$M_2, \text{app}/M_2, \text{real}$				
BSA	NaCl	11.7	-0.68	0.90	7.17	1.007	1.007	2.42	19.2	1.019	1.019				
BSA	NaCl	1.17	-3.26	0.90	3.43	1.003	1.003	2.49	9.5	1.010	1.010				
BSA	NaSCN	16.2	-1.38	0.85	18.9	1.019	1.019	1.76	39.3	1.039	1.039				
BSA	NaSCN	1.62	-5.07	0.85	7.0	1.007	1.007	1.76	14.4	1.014	1.014				
BSA	Urea	480	-1.74	0.62	1.040	2.04	2.04	0.92	1.537	2.54	2.54				
NaDNA	HgCl ₂	13.6	-37.2	0.59	196	1.20	1.20	1.65	557	1.56	1.56				

(a) Calculated according to equation (15).

(b) Calculated according to equation (9).

In every case, the apparent molecular weight turns out to be somewhat higher than the true value of M_2 . Binding of NaCl and NaSCN to BSA, however, result in an effect smaller than the usual experimental error in both X-ray scattering and light scattering. This permits treatment of these systems as pseudo two-component ones. The opposite is true for BSA-urea and NaDNA-HgCl₂, where the effect of binding results in apparent molecular weights up to 2.5 times larger than the true value of M_2 . This is reflected also in a significant effect on the slopes of the concentration dependent curves. Deviations of such magnitude from M_2 can be used to advantage to determine the extent of preferential binding of component 1 to component 2 (Ewart, Roe, Debye and McCartney, 1946).

Case 2: Preferential binding of solvent. The contribution of binding to the factor D represents in reality preferential binding and \bar{v} can be positive or negative, depending on whether there is an excess of component 1 or component 0 in the vicinity of molecules of 2. This is due to the fact that the free energy of binding, ΔF^b , is the difference between the free energies of interaction of 2 with 1 and of 2 with 0:

$$\Delta F^b = \Delta F^{12} - \Delta F^{02} \quad (13)$$

But:

$$\frac{\partial \mu_2^b}{\partial m_1} = \frac{\partial^2 \Delta F^{12}}{\partial m_1 \partial m_2} - \frac{\partial^2 \Delta F^{02}}{\partial m_1 \partial m_2} \quad (14)$$

and

$$A_{12} = \frac{M_1}{M_2 RT} \frac{\partial \mu_2^e}{\partial C_1} = \frac{-10^3}{M_2 \Sigma v_1} \frac{\bar{v}}{m_1} (\Sigma v_1 + A_{11} C_1) \quad (15)$$

Thus, if ΔF^{02} is larger than ΔF^{12} , ΔF^b is positive, A_{12} is positive and \bar{v} is negative, indicating a deficiency of component 1 in the immediate vicinity of molecules 2, or, in other words, hydration of component 2. This leads to the intercept of equation (9) being higher than $1/M_2$.

Now,

$$\bar{v} = \Sigma v_1 \left(\frac{\partial m_1}{\partial m_2} \right)_{\mu_1},$$

and

$$\left(\frac{\partial m_0}{\partial m_2} \right)_{\mu_0} = - \frac{m_0}{m_1} \left(\frac{\partial m_1}{\partial m_2} \right)_{\mu_1} \quad (16)$$

giving the number of moles of solvent bound per mole of macromolecule.

Using these equations the reported small-angle X-ray scattering on DNA in the presence of NaCl and NaBr (Luzzati, Nicolaieff and Masson, 1961) has been examined with the aim of establishing the excess of water present in the neighborhood of the DNA molecules, i.e. its degree of hydration. At the level of resolution of small-angle X-ray scattering, DNA is found to

have the shape of infinitely long rods (see Fig. 4). Since, under these circumstances, it is impossible to obtain the molecular weight, M_2 , the quantity of interest is the mass per unit length, M_2/L_2 , where L_2 is the total contour length of the DNA molecule. The value of M_2/L_2 reported at zero ionic strength is 197 mass units per Å. The interaction term, D , is then given by the relation:

$$D = \frac{(M_2/L_2)_{\text{experimental}}}{197} - 1 \quad (17)$$

Application of equations (12), (15), (16) and (17) to the literature data as a function of salt concentration leads to the results of Table 2. In both salts, D

TABLE 2. PREFERENTIAL BINDING OF WATER BY DNA

m_1	$M_2/L_2^{(a)}$	$D^{(b)}$	$\bar{v}^{(c)}$	$\partial m_0/\partial m_2^{(d)}$ (moles H ₂ O/Å DNA)
<i>NaCl</i>				
3.0	130	-0.341	-0.42	7.1
2.0	151	-0.233	-0.25	6.7
1.0	173	-0.121	-0.14	7.4
0.5	180	-0.084	-0.09	10.0
0.2	193	-0.020	-0.022	5.9
<i>NaBr</i>				
1.48	123	-0.377	-0.22	7.8
1.09	139	-0.297	-0.17	8.4
0.74	166	-0.159	-0.09	6.6

(a) Data taken from Luzzati, Nicolaieff and Masson (1961), recalculated into mass units.

(b) Calculated according to equation (17).

(c) Calculated according to equation (12); $\Sigma \nu_1$ was taken as 1, since binding of entire salt is considered, rather than of particular ions.

(d) Calculated according to equation (16).

is found to become progressively more negative with increasing salt concentration, indicating a net repulsion of the salt by the nucleic acid. This is reflected in the values of \bar{v} , which show that the difference between the bulk salt concentration and that in the immediate neighborhood of the macromolecules becomes progressively larger as the salt concentration increases. This indicates that the macromolecule is interacting preferentially with the solvent, or, in terms of a specific molecular model, a layer of water impenetrable to salt is formed around the DNA molecule. The degree of hydration ($\partial m_0/\partial m_2$) is found to be identical within experimental error for the two salts; it has values of 0.68 g H₂O/g DNA in NaCl and 0.70 g H₂O/g DNA in NaBr. This is in good agreement with the values calculated in the literature (0.68 g H₂O/g DNA) (Luzzati, Nicolaieff and Masson, 1961) using a geometric analysis of the electron density of a specific model rather than a thermodynamic approach to the problem.

Case 3: Protein-protein interaction. Here both components 1 and 2 are macromolecular in nature. The problem consists in obtaining values of A_{12} and \bar{v} , from an analysis of the slope and of the parameter D . In order to accomplish this it is necessary to possess a knowledge of M_1 , M_2 , A_{11} and A_{22} . This is readily obtainable from scattering data on the two components, each studied individually under conditions identical with those at which the interaction takes place. The constants A_{11} and A_{22} are obtained directly from the slopes of these scattering curves and M_1 and M_2 from their intercepts. Substitution of these parameters and of the value of α into equation 9 permits one to obtain D and A_{12} from the difference between this calculated curve and the experimental one obtained on a mixture of 1 and 2 under conditions of interaction. The value of A_{12} shows the strength of the attraction between components 1 and 2 and is quite general in nature, since its calculation involves no models nor any assumptions on the nature of the interaction at the molecular level. If a model is then assumed, involving molecular complex formation between 1 and 2, the stoichiometry of the interaction may be obtained from equation (15) by calculating \bar{v} , which is the average number of molecules of protein 1 bound to a molecule of protein 2. This, of course, can then readily give the equilibrium constant of the interaction and the usual thermodynamic parameters.

As an example, let us carry out this type of calculation on the very elegant study described by Pepe and Singer (1959), who investigated by light scattering the complexing of a univalent antigen, Ag (component 1) with a divalent antibody, Ab (component 2). The successive steps involved in this calculation are depicted in Fig. 2.* The data of Pepe and Singer are represented in this figure by curves 1 to 4. These give, in turn, the scattering of the Ag-Ab complexing mixture (curve 1), the antibody mixed with bovine mercaptalbumin, BMA (which has the same molecular properties as the antigen but does not complex with the antibody) (curve 2), the Ag-Ab mixture with no interaction (curve 3, deduced) and pure BMA (curve 4). The necessary information for rigorous formal application of the three-component theory analysis was obtained as follows. All the curves were recalculated first as turbidities, since it is the scattered intensities of the various components which are additive, and not the parameters $Hc/\Delta\tau$. Point by point subtraction of the turbidities of curve 4 from those of curve 2 gives the turbidity as a function of concentration for free antibody. This, calculated as $Hc/\Delta\tau$, is curve 5; its slope is A_{22}/M_2 , needed to evaluate the first concentration dependent term of equation (9); its intercept is $1/M_2$. When the turbidities of this last curve (curve 5) are subtracted from those of curve 3 (Ag-Ab mixture with no interaction), the result is the turbidity of pure antigen (component 1)

* This case is somewhat complicated by the fact that no scattering data were available on Ab in the pure state. As a result several extra steps were necessary to arrive at the necessary values of A_{22} and M_2 .

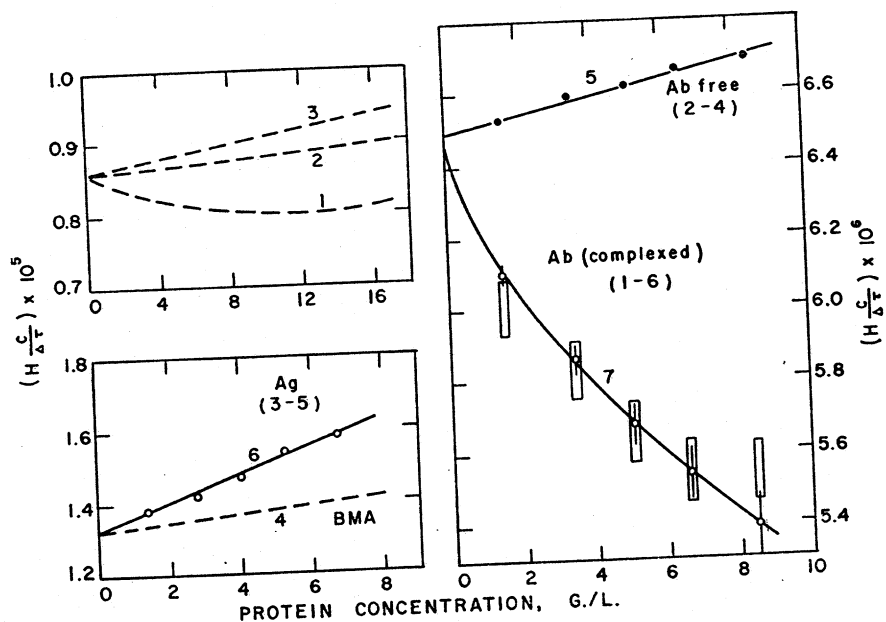


FIG. 2. Three component analysis of light scattering data for the interaction of two proteins (Pepe and Singer, 1959).

at the same conditions at which interaction occurs; plotting this as $Hc/\Delta\tau$ (curve 6) yields $1/M_1$ (intercept) and A_{11}/M_1 (slope), needed in the evaluation of D and the second concentration dependent term of equation (9). Subtracting the turbidities of this curve from the turbidities of curve 1 results in the turbidities due to antibody alone (component 2), when it is in a state of interaction with component 1. This result is represented in terms of $Hc/\Delta\tau$ by the rectangles shown on curve 7. The deviation of these points from the $Hc/\Delta\tau$ values of non-interacting antibody (solid circles of curve 5) is a measure of the thermodynamic interaction between Ab and Ag. In curve 7 the presence of component 1 is manifested only through the thermodynamic interaction terms, i.e. by the values of A_{12} ; it does not make any contribution to the measured molecular weight, nor is any assumption involved about the nature of the interaction, i.e. no models are postulated. The sharp decrease of $Hc/\Delta\tau$ with concentration found in curve 7 manifests the presence of a strong attractive force between components 1 and 2. From the ratio of the $Hc/\Delta\tau$ values of curve 7 to $1/M_2$, the factor D is obtained within the approximation of neglect of the contribution of A_{12} to the slope. Use of equations (12) and (15) yields approximate values of A_{12} and \bar{v} . Successive repetition of this process results in exact values of A_{12} and \bar{v} for each concentration point. If the assumption is made that the interaction is one of complexing (which is

true in this particular case), the intrinsic binding constant of protein 1 to protein 2, k_{12} , may be evaluated as

$$k_{12} = \frac{\bar{v}}{nm'_1 - \bar{v}m'_1} \quad (18)$$

where n is the total number of binding sites on component 2 and m'_1 is the molar concentration of unbound component 1, namely $m'_1 = m_1 - \bar{v}m_2$. Using the method described here, the value of k_{12} obtained was found to be $(1.85 \pm 0.25) \times 10^3$ l./mole which is in good agreement with the value deduced by Pepe and Singer. The points calculated at each concentration using this value are represented by the open circles of curve 7 of Fig. 2. It is interesting to note that here, contrary to the usual situation in light scattering, the concentrations of *both* components 1 and 2 extrapolate to zero. As a result, curve 7 extrapolates to the true value of $1/M_2$, the system reducing to a two-component one at infinite dilution.

In this section an attempt has been made to show by a series of examples how light scattering and small-angle X-ray scattering may be used to determine the thermodynamics of interactions. In the next section we shall demonstrate how a combination of these two techniques can yield considerable information on the geometry of biological systems.

GEOMETRY OF SCATTERING

The thermodynamic treatment described in the previous section was based on the assumption that either the scattering data were extrapolated to zero angle or that the particles were small relative to the wavelength of the incident radiation; the latter situation prevails in the case of light scattering of most globular proteins. In the case of particles whose dimensions are large compared to the wave length, interference effects occur between individual scattering elements within a particle with the result that the scattering envelope is asymmetric and the intensity diminishes as the angle formed between the scattered and incident beams increases. This information is the basis of particle geometry determination.

Debye (1915) has shown for both light scattering and small-angle X-ray scattering that the angular dependence of the scattering of a particle of any shape, averaged over all orientations, is given by (see also Guinier, 1956):

$$P(\theta) = \frac{1}{N^2} \sum_k^N \sum_j^N \frac{\sin 2\pi sr_{kj}}{2\pi sr_{kj}}$$

$$s = \frac{2}{\lambda} \sin \frac{\theta}{2}$$

where N is the total number of scattering elements in the particle, r_{kj} is the distance between elements k and j , λ is the wavelength of the incident radiation and θ is the angle formed between the incident and scattered beams. Using this equation, the angular dependence of the scattering of particles of various shapes has been calculated. (These will not be discussed here, the reader being referred to references cited at the beginning of this article.) Guinier (1939) has shown that at very small angles the scattering intensity as a function of angle, $i(s)$, is closely described by

$$i(s) = i(0) e^{-\frac{1}{3}\pi^2 R^2 s^2} \quad (20)$$

where R is the radius of gyration of the particle. This is known as the Law of Guinier and it is independent of the shape of the particle. In this angular region, a plot of $\log i(s)$ as a function of s^2 approaches linearity; R is obtained from the limiting slope, while the intercept yields $i(0)$ from which the molecular weight of the particle and thermodynamic properties of the system may be obtained as described above.

At higher values of s , $i(s)$ deviates from equation (20), the curve becomes highly dependent on the shape of the particle and, in some cases, passes through maxima and minima. Such data may be treated by specific equations derived for particles of various shapes. At large values of s , i.e. when s is large with respect to the reciprocal of the smallest dimension of the particle, the scattering intensity becomes proportional on the average to the fourth power of the scattering angle (Porod, 1951):

$$s^4 i(s) \approx \frac{1}{8\pi^3} (\rho_k - \rho_0)^2 N_k S_k \quad (21)$$

where ρ_k is the electron density of the particle, ρ_0 that of the solvent, N_k is the number of particles and S_k is the surface area of one particle. Equation (21) is valid only when particles k have a uniform electron density. This angular region may be used to determine the surface area of the scattering molecules. We shall show now by the example of ribonucleic acid (RNA) and β -lactoglobulin how a combination of light scattering and small-angle X-ray scattering can be used to advantage to obtain detailed information on the geometry of a complicated molecule.

Ribonucleic Acid

The high molecular weight RNA fraction of ascites tumor cells has been studied under identical conditions (pH 6.8, $\Gamma/2 = 0.14$ NaCl; 0.01 Na phosphate) by light scattering (Kronman, Timasheff, Colter and Brown, 1960) and small-angle X-ray scattering (Timasheff, Witz and Luzzati, 1961). For the sake of comparison, the results of the two techniques have been plotted together on Fig. 3. The light scattering data obtained at a single

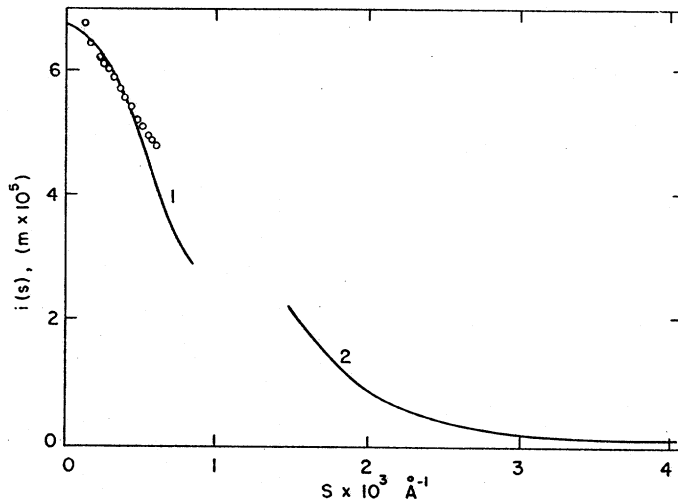


FIG. 3. Light scattering and small-angle X-ray scattering of high molecular weight RNA. Circles: light scattering data; curve 1: Guinier plot in closest agreement with experimental data; curve 2: Excess small-angle X-ray scattering over contribution of internal structure. The intensity (ordinate) is expressed in terms of apparent molecular weight in electrons.

concentration are plotted as the circles in Fig. 3. The solid line (curve 1) is a Guinier plot which fits best these data. Its analysis results in a Z-average radius of gyration of $315 \pm 35 \text{ \AA}$ and a weight average molecular weight of 1.32×10^6 (or 6.74×10^5 electrons). At low angles, the experimental points are found to follow reasonably well the Guinier Law (equation (20)); at higher angles, an upward deviation becomes apparent. These light scattering data indicate that the RNA molecule is a rather compact particle with a maximal dimension close to 1000 \AA . Ultracentrifugal analysis has shown this RNA to be a mixture of molecules of two sizes, one (comprising 63 per cent of the total RNA) having a molecular weight of 1.9×10^6 , the other (37 per cent) a molecular weight of 3.2×10^5 .

Small-angle X-ray scattering measurements on this material resulted in the data plotted on Fig. 4.* The open circles represent the experimental points on freshly prepared RNA. The data were analyzed by comparison with theoretical curves for particles of various shapes. It was found that for s greater than 0.01 \AA^{-1} , RNA behaves like a rigid rod, with a cross-sectional radius of gyration of 8.2 \AA and a mass per unit length in reasonable agreement with a Watson-Crick double helix. The solid line is the calculated theoretical curve

* The scattering intensities expressed in Fig. 4 by the symbol $j_n(s)$ were obtained using an infinitely long slit optical system. These values can be reduced to the point source optics intensities, $i(s)$, used throughout this paper, by mathematical transformation (see Guinier and Fournet, 1955, or Luzzati, 1960).

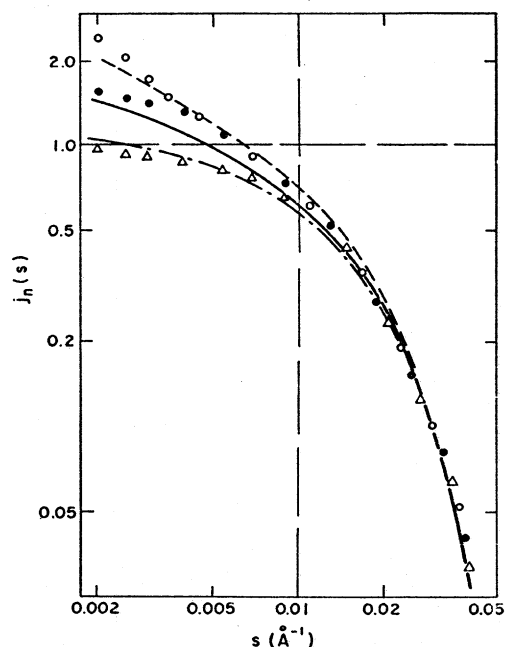


FIG. 4. Small-angle X-ray scattering of RNA. Open circles: fresh RNA; filled circles: same after 2 days at room temperature; triangles: same after 18 days at room temperature.

for a rigid rod having a length infinite with respect to the maximal resolution of the experiment (Porod, 1948; Luzzati, 1960). At values of s below 0.01\AA^{-1} the points deviate upward from this curve and fit rather well the theoretical curve for a zigzag chain of short rigid rods, the length of each rod being *ca.* 85\AA . The theoretical curve for this case is shown by the dashed line (Hermans and Hermans, 1958; Luzzati and Benoit, 1961). Slow thermal degradation of the RNA resulted in a scattering pattern in which the intensity at $s < 0.01 \text{\AA}^{-1}$ slowly decreased with time until it reached final values given by the triangles. These correspond well to the theoretical curve (dot-dashed line) for independent rods with a length of *ca.* 85\AA and a cross-sectional radius of gyration of 8.2\AA . From these X-ray scattering data it was concluded that the structure of this RNA under conditions close to physiological is that of a zigzag chain of rods, *ca.* 85\AA in length and a cross section equal to that of a Watson-Crick double helix.

At values of s smaller than 0.003\AA^{-1} , the experimental data on fresh RNA are seen to rise above the theoretical curve for a broken-rod. This can be interpreted as the contribution of the tailing-off of the scattering from the molecule as a whole, i.e. the same entity as that observed by light scattering. When the theoretical scattering for the detailed structure of the molecule

(dashed line) was subtracted from the total observed scattering, the remainder gave the angular dependence shown by curve 2 of Fig. 3. The tendency of this last curve toward the light scattering experimental points indicates consistency between the two sets of data.

The radius of gyration of the molecule, as observed by light scattering, was then calculated from the small-angle X-ray scattering data. According to Hermans and Hermans (1958) the radius of gyration, R , of a zigzag chain is:

$$R^2 = (A^2/6)(N - 1 + 1/2N) \quad (22)$$

where A is the length of the subunit (85 Å in this case), and N is the number of subunits per chain. Assuming that RNA is a long broken Watson-Crick double helix, the numbers of subunits (N) in the two components are 106 and 18, respectively, resulting in radii of gyration of 355 Å and 143 Å (equation (22)). From these values and the ultracentrifugal composition, we obtain $\bar{R}_z = 340$ Å, which is in reasonable agreement with the light scattering value

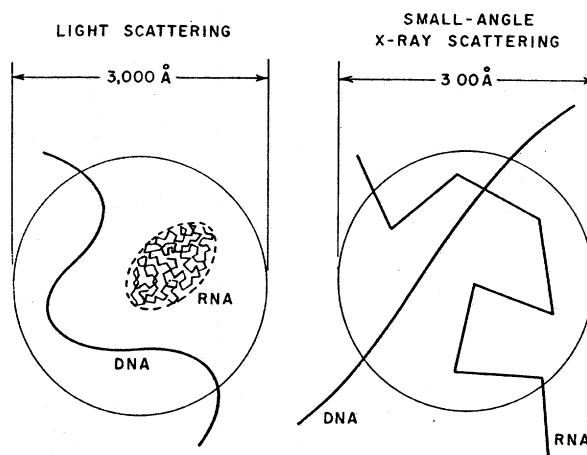


FIG. 5. Structures of RNA and DNA as seen at the levels of resolution of light scattering and small-angle X-ray scattering.

of 315 ± 35 Å. This example has shown how the different orders of resolution of the two scattering techniques can be used to advantage to obtain simultaneously the overall and detailed internal structures of a large biological molecule. This is depicted in Fig. 5, which shows schematically the structure of RNA as seen by light scattering and small-angle X-ray scattering. For the sake of comparison, a molecule of DNA is also shown. It is obvious that, while in X-ray scattering DNA appears as an infinitely long rigid rod, in light scattering its behavior is closer to that of a worm-like chain. This is indeed the situation found experimentally.

β -Lactoglobulin A

The second example is that of a small globular protein which assumes various degrees of aggregation as a function of pH. A detailed study of this protein (Timasheff and Townend, 1961) has shown that, while in the isoelectric region it has a molecular weight of 36,000, as the pH is lowered, it first undergoes a reversible tetramerization (molecular weight 144,000), and then a dissociation in half (molecular weight 18,000). Green and Aschaffenburg (1959) have further shown by X-ray crystallography that the 36,000 molecular weight species has the structure of two identical touching spheres.

A small-angle X-ray scattering study has been carried out on this protein under isoelectric conditions as well as in the pH zone in which it undergoes tetramerization (Timasheff, Witz and Luzzati, to be published). The molecular weights found under these conditions were essentially identical with those measured by light scattering. The radii of gyration are $21.7 \pm 0.4 \text{ \AA}$ for the isoelectric species and $34.4 \pm 0.4 \text{ \AA}$ for the tetramer. These values were compared with theoretical ones calculated for a number of models. The isoelectric value of the radius of gyration is found to be consistent with a molecule not much different from the double sphere model of Green and Aschaffenburg (1959), deduced from crystallographic studies.

In the case of the tetramer, thermodynamic analysis of the light scattering data (equation (11)) showed that the aggregate must be in the shape of a closed ring. The calculated radius of gyration for such a ring of four Green and Aschaffenburg units is 36.2 \AA ; this is in good agreement with the experimentally found value of 34.4 \AA . Considering the approximations made in the selection of simple geometric forms for molecules which in reality must be irregular in shape, this degree of agreement can be considered as complete verification by the small-angle X-ray scattering geometric analysis of the deduction reached from the light scattering thermodynamic study.

While the principal shape parameter obtained from scattering studies of interacting systems is the Z-average radius of gyration, small-angle X-ray scattering is also capable of yielding the surface to volume ratio, the volume and the degree of internal hydration of a molecule. In the case of interacting systems, however, these become rather complicated average quantities and will not be discussed here.

CONCLUSION

The present analysis of light scattering and small-angle X-ray scattering data has shown these two techniques to be powerful tools for the understanding of interacting biological systems. While each is capable of yielding information on the thermodynamics and geometry of the interactions, it is through a combination of the two that the most powerful structural analysis of biological complexes in solution can be obtained.

REFERENCES

- BEEMAN, W. W., KAESBERG, P., ANDEREGG, J. W. and WEBB, M. B. (1957) In *Handbuch der Physik*, Flügge, S., editor, vol. 32, p. 321.
- BRINKMAN, H. C. and HERMANS, J. J. (1949) *J. Chem. Phys.* **17**, 574.
- DEBYE, P. (1915) *Ann. Physik* [4], **46**, 809.
- DEBYE, P. (1947) *J. Phys. and Colloid Chem.* **51**, 18.
- DOTY, P. and STEINER, R. F. (1952) *J. Chem. Phys.* **20**, 85.
- EWART, R. H., ROE, C. P., DEBYE, P. and MCCARTNEY, J. R. (1946) *J. Chem. Phys.* **14**, 687.
- FLÜGGE, S., editor (1957) *Handbuch der Physik*, vol. 32. Springer, Berlin.
- FOURNET, G. (1951) *Acta Cryst.* **4**, 293.
- GEIDUSCHEK, E. P. and HOLTZER, A. (1948) *Advances in Biol. and Med. Phys.* **6**, 431.
- GREEN, D. W. and ASCHAFFENBERG, R. (1959) *J. Mol. Biol.* **1**, 54.
- GUINIER, A. (1939) *Ann. Phys.* **12**, 161.
- GUINIER, A. (1956) *Theorie et Technique de la Radiocristallographie*. Dunod, Paris.
- GUINIER, A. and FOURNET, G. (1955) *Small-Angle Scattering of X-rays*. Wiley, New York.
- HERMANS, J. JR and HERMANS, J. J. (1958) *J. Phys. Chem.* **62**, 1543.
- KATZ, S. (1952) *J. Amer. Chem. Soc.* **74**, 2238.
- KAY, C. M. and EDSALL, J. T. (1956) *Arch. Biochem. Biophys.* **65**, 354.
- KIRKWOOD, J. G. and GOLDBERG, R. J. (1950) *J. Chem. Phys.* **18**, 54.
- KIRKWOOD, J. G. and TIMASHEFF, S. N. (1956) *Arch. Biochem. Biophys.* **65**, 50.
- KRONMAN, M. J., TIMASHEFF, S. N., COLTER, J. S. and BROWN, R. A. (1960) *Biochim. Biophys. Acta* **40**, 410.
- LUZZATI, V. (1960) *Acta Cryst.* **13**, 939.
- LUZZATI, V. and BENOIT, H. (1961) *Acta Cryst.* **14**, 297.
- LUZZATI, V., NICOLAIEFF, A. and MASSON, F. (1961) *J. Mol. Biol.* **3**, 185.
- OSTER, G. (1948) *Chem. Revs.* **43**, 319.
- PEPE, F. A. and SINGER, S. J. (1959) *J. Amer. Chem. Soc.* **81**, 3878.
- POROD, G. (1948) *Acta Phys. Austriaca* **2**, 255.
- POROD, G. (1951) *Kolloid-Z.* **124**, 83.
- SCATCHARD, G., COLEMAN, J. S. and SHEN, A-L. (1957) *J. Amer. Chem. Soc.* **79**, 12.
- STOCKMAYER, W. H. (1950) *J. Chem. Phys.* **18**, 58.
- TANFORD, C. (1961) *Physical Chemistry of Macromolecules*. Wiley, New York.
- TIMASHEFF, S. N. and COLEMAN, B. D. (1960) *Arch. Biochem. Biophys.* **87**, 63.
- TIMASHEFF, S. N., DINTZIS, H. M., KIRKWOOD, J. G. and COLEMAN, B. D. (1957) *J. Amer. Chem. Soc.* **79**, 782.
- TIMASHEFF, S. N. and KRONMAN, M. J. (1958) *Arch. Biochem. Biophys.* **83**, 60.
- TIMASHEFF, S. N. and TOWNEND, R. (1961) *J. Amer. Chem. Soc.* **83**, 464, 470.
- TIMASHEFF, S. N., WITZ, J. and LUZZATI, V. (1961) *Biophys. J.* **1**, 526.
- TOWNEND, R. and TIMASHEFF, S. N. (1960) *J. Amer. Chem. Soc.* **82**, 3168.
- VAN DE HULST, H. C. (1957) *Light Scattering by Small Particles*. Wiley, New York.